

Thermodiffusion in concentrated ferrofluids: Experimental and numerical results on magnetic thermodiffusion

Lisa Sprenger,^{a)} Adrian Lange, and Stefan Odenbach

Institute of Fluid Mechanics, Chair of Magnetofluidynamics, Measuring and Automation Technology, TU Dresden, 01062 Dresden, Germany

(Received 3 July 2013; accepted 20 January 2014; published online 10 February 2014)

Ferrofluids consist of magnetic nanoparticles dispersed in a carrier liquid. Their strong thermodiffusive behaviour, characterised by the Soret coefficient, coupled with the dependency of the fluid's parameters on magnetic fields is dealt with in this work. It is known from former experimental investigations on the one hand that the Soret coefficient itself is magnetic field dependent and on the other hand that the accuracy of the coefficient's experimental determination highly depends on the volume concentration of the fluid. The thermally driven separation of particles and carrier liquid is carried out with a concentrated ferrofluid ($\varphi = 0.087$) in a horizontal thermodiffusion cell and is compared to equally detected former measurement data. The temperature gradient (1 K/mm) is applied perpendicular to the separation layer. The magnetic field is either applied parallel or perpendicular to the temperature difference. For three different magnetic field strengths (40 kA/m, 100 kA/m, 320 kA/m) the diffusive separation is detected. It reveals a sign change of the Soret coefficient with rising field strength for both field directions which stands for a change in the direction of motion of the particles. This behaviour contradicts former experimental results with a dilute magnetic fluid, in which a change in the coefficient's sign could only be detected for the parallel setup. An anisotropic behaviour in the current data is measured referring to the intensity of the separation being more intense in the perpendicular position of the magnetic field: $S_{T\parallel} = -0.152 \text{ K}^{-1}$ and $S_{T\perp} = -0.257 \text{ K}^{-1}$ at $H = 320 \text{ kA/m}$. The ferrofluid-dynamics-theory (FFD-theory) describes the thermodiffusive processes thermodynamically and a numerical simulation of the fluid's separation depending on the two transport parameters ξ_{\parallel} and ξ_{\perp} used within the FFD-theory can be implemented. In the case of a parallel aligned magnetic field, the parameter can be determined to $\xi_{\parallel} = \{2.8; 9.1; 11.2\} \times 10^{-11} \cdot D_{\parallel} \text{ kg}/(\text{A}^2\text{m})$ for the different field strengths and in dependence on the magnetic diffusion coefficient D_{\parallel} . An adequate fit in the perpendicular case is not possible, by $\xi_{\perp} = 1 \times 10^{-17} \text{ kg}/(\text{Am}^2)$ a rather good agreement between numerical and experimental data can be found for a field strength of 40 kA/m, a change in the coefficient's sign in the perpendicular setup is not numerically determinable via this theory. The FFD-theory is only partly applicable to calculate the concentration profile in concentrated magnetic fluids established due to a temperature gradient and magnetic field applied. © 2014 AIP Publishing LLC. [<http://dx.doi.org/10.1063/1.4864107>]

I. INTRODUCTION

The physical properties of magnetic fluids, as being composed of a carrier liquid and magnetic nanoparticles, can be generally influenced by applying a magnetic field to a volume of the fluid. Thermodiffusive properties of these fluids, describing the separation of carrier liquid and particles due to the exposure of the fluid to a temperature gradient, are of main interest in the present work. On

^{a)} Author to whom correspondence should be addressed. Electronic mail: Lisa.Sprenger@tu-dresden.de

one hand previous works on thermodiffusion for zero and non-zero magnetic fields¹⁻⁴ point out that thermally induced particle transport in colloidal suspensions is far more intense than thermodiffusion in binary fluid mixtures. Which means that the Soret coefficient S_T in magnetic fluids is approximately two orders of magnitude higher than in fluid mixtures.^{5,6} On the other hand these investigations^{3,7} emphasise that the volume concentration of the fluids has an impact on the separation process which cannot be neglected. The Soret coefficient is expected to be concentration-dependent with decreasing values for the coefficient by increasing particle concentration.⁷

Especially, in the case of magnetic separation processes, i.e., in a situation where beside the temperature gradient an external, homogeneous magnetic field is applied across the layer of magnetic fluid, the thermodiffusive particle transport is expected to be even more intense than in the non-magnetic case leading to Soret coefficients of about $S_{T_m} = |0.6| \text{ K}^{-1}$ which is approximately 4 times larger than the non-magnetic Soret coefficient.^{2,4} To measure the magnetic separation different research groups developed two different equipments, namely, the Forced-Rayleigh-Scattering (FRS)⁸⁻¹⁰ and a horizontal thermodiffusion cell.^{4,11} In the first method the layer of magnetic fluid is exposed to the interference pattern of two crossed laser beams. This leads to a regular temperature distribution and thereby induces the thermal separation process. The thermodiffusion cell of the second method consists of a thin area where separation takes place, positioned between two grids and two fluid reservoirs positioned above and below the separation area. Different temperatures at the upper and lower boundary of the fluid cell establish a constant temperature gradient over the fluid volume. The Soret coefficient can be retrieved from the separation signal's slope. The signal detected is the difference of the relative concentration in the lower and upper reservoir. The reduced height of the separation area within the double grid suppresses thermomagnetic convection, which could otherwise arise even in a thermally stable setup.^{4,12} Convective motion for the system is thereby described by the magnetic Rayleigh number (Ra_m)¹²

$$Ra_m = \frac{\mu_0 K^2 \Delta T^2 h_g^2}{\kappa \eta}, \quad (1)$$

with μ_0 denoting the magnetic permeability of vacuum, ΔT the temperature difference at the grid's boundaries, h_g the grid's height, K the pyromagnetic coefficient of the fluid, κ the temperature conductivity, and η the viscosity. By using the double-layer grid the temperature difference in the experiments described in Sec. III A is reduced from 14 K to 1.5 K and the cell's height from 14 mm to the grid's height of 1.5 mm which reduces the magnetic Rayleigh number by a factor 8×10^3 .

The determination of the Soret coefficient in the horizontal diffusion cell is based on a phenomenological approach resulting in the following equation of the diffusive mass flux

$$\vec{j} = -\rho D_m \vec{\nabla} c - \rho c(1-c) D_m S_{T_m} \vec{\nabla} T, \quad (2)$$

with c denoting the mass concentration of nanoparticles. D_m denotes the magnetic field dependent diffusion coefficient, and S_{T_m} the magnetic field dependent Soret coefficient.⁴ If one of the two coefficients is referred to in a specific orientation of the magnetic field in the following, the index "m" will be substituted by the orientation "||" or "⊥." Equation (2) is derived from the mass flux in the non-magnetic case⁴ and it is assumed that the magnetic contributions to the flux can be accounted for by the magnetic contributions to its transport parameters D and S_T . The change in concentration over time is calculated by $\frac{\partial c}{\partial t} = -\frac{\vec{\nabla} \cdot \vec{j}}{\rho}$. Considering the geometric characteristics of the experimental setup, Eq. (2) results in the separation curve

$$\frac{c_{lo} - c_{up}}{c_0} = \frac{4}{h - h_g} D_m S_{T_m} \frac{\Delta T}{h} t \quad (3)$$

describing the measured signal. For the determination of the Soret coefficient, its slope can be fitted to the experimentally sampled relative concentration difference.^{3,4} The concentration in the lower (upper) fluid reservoir $c_{lo(up)}$ is normalised by the homogeneous initial concentration c_0 , h denotes the height of the fluid cell, h_g the height of the separation area, and ΔT is the temperature difference applied to the fluid container.⁴ To derive Eq. (3) from Eq. (2) a couple of assumption have to be made according to former experiments:^{3,4} (1) the fluid is assumed dilute ($1 - c \approx 1$); (2) the term of molecular diffusion can be neglected due to its order of magnitude being 2 orders smaller than

the one of the second term; (3) the concentration gradient is assumed constant; (4) $\vec{\nabla} \cdot \vec{j}$ can be described via $\vec{n} \frac{2}{h-h_g} \cdot \vec{j}$, with \vec{n} being the normal vector at the two grid sides; (5) $c(t=0) = c_0$. Based on these assumptions the differential equation which has to be solved in each fluid reservoir is $\frac{dc}{dt} = -\frac{2}{h-h_g} \vec{n} \cdot (-D_m S_{Tm} c \vec{\nabla} T)$ and its solution then leads directly to Eq. (3).³

Besides the phenomenological ansatz the diffusive mass flux can also be described by the thermodynamical approach of the ferrofluidynamics-theory (FFD-theory).¹³⁻¹⁶ The mass flux

$$-\vec{j}_1 = \xi_1 \vec{\nabla} T + \xi \vec{\nabla} \tilde{\mu}_c + \xi_{\parallel} \vec{M} (\vec{M} \vec{\nabla}) \tilde{\mu}_c + \xi_{\perp} (\vec{M} \times \vec{\nabla}) \tilde{\mu}_c \quad (4)$$

thereby consists of four different diffusion-driving terms: the gradient in temperature, and three terms based on the chemical potential $\tilde{\mu}_c$ of the fluid related to the applied magnetic field \vec{H} by the fluid's magnetisation \vec{M} . The last two account for the magnetic influence in a setup with a magnetic field aligned parallel or perpendicular to the temperature gradient.^{13,16} These four terms are linked with the transport parameters ξ_1 , ξ , ξ_{\parallel} , and ξ_{\perp} which have to be determined experimentally to evaluate their actual relevance in the diffusive mass flux in the magnetic setup.^{13,16} The different terms intend to include any effect that the application of a magnetic field could have on the diffusive mass flux since a microscopic understanding of the transport mechanism could not be established so far. Regarding the relevant flux-driving terms in Eq. (4) an ansatz for the chemical potential $\tilde{\mu}_c$ is required containing a non-magnetic part μ_c and a magnetic part,¹⁷ standing for $-\mu_0 \int_0^H \frac{\partial M}{\partial \rho_1} d\vec{H}$ according to Lange.¹⁶ It reads^{16,18,19}

$$\tilde{\mu}_c(\rho, \rho_1, T, H) = \mu_c(\rho, \rho_1, T) - \frac{k_B T \varphi}{\rho_1 V} \left[\ln \frac{\sinh(\alpha)}{(\alpha)} \right], \quad (5)$$

with k_B being the Boltzmann constant, T the fluid's temperature, V the volume of one nanoparticle, φ the volume concentration of the nanoparticles, and α being the Langevin parameter

$$\alpha = \frac{\mu_0 M_d V H}{k_B T}, \quad (6)$$

where M_d denotes the bulk magnetisation of the nanoparticles' material and μ_0 the permeability of the vacuum.²⁰ The fluid's density is taken account for by ρ , $\rho_1 = c \cdot \rho$ denotes the product of the nanoparticles' mass concentration and the fluid's density. The non-magnetic part of the chemical potential reads^{16,21}

$$\mu_c(\rho, \rho_1, T) = \frac{k_B T}{m_1} \ln \frac{\rho_1}{\rho} - \frac{k_B T}{m_2} \ln \left(1 - \frac{\rho_1}{\rho} \right) + const \quad (7)$$

with m_1 and m_2 denoting the mass of one molecule of the fluid's particles and the carrier liquid. The *Ansätze* in Eqs. (5) and (7) entered in Eq. (4) finally lead to the explicit diffusive mass flux

$$\begin{aligned} -\vec{j} &= \xi_1 \vec{\nabla} T + \frac{\partial \tilde{\mu}_c}{\partial T} \left(\xi \vec{\nabla} T + \xi_{\parallel} \vec{M} (\vec{M} \vec{\nabla}) T + \xi_{\perp} (\vec{M} \times \vec{\nabla}) T \right) \\ &+ \rho \frac{\partial \tilde{\mu}_c}{\partial \rho_1} \left(\xi \vec{\nabla} c + \xi_{\parallel} \vec{M} (\vec{M} \vec{\nabla}) c + \xi_{\perp} (\vec{M} \times \vec{\nabla}) c \right) \\ &- \mu_0 \frac{\partial M}{\partial \rho_1} \left(\xi \vec{\nabla} H + \xi_{\parallel} \vec{M} (\vec{M} \vec{\nabla}) H + \xi_{\perp} (\vec{M} \times \vec{\nabla}) H \right), \end{aligned} \quad (8)$$

the first line denoting thermophoresis, the second line denoting diffusiophoresis, and the third line denoting magnetophoresis.¹⁶ H denotes the magnetic field strength. The diffusion equation for the approach in Eq. (8) is again derived from $\frac{\partial c}{\partial t} = -\frac{\vec{\nabla} \cdot \vec{j}}{\rho}$. It will be solved numerically in Sec. IV B leading to a concentration profile over the considered fluid volume and will be fitted to the experimental separation curves to obtain the magnetic Soret coefficient.

Beside the numerical determination an analytical approximation of the magnetic Soret coefficient retrieved from the thermodynamical approach is given by Lange¹⁶ for the two different field orientations. To obtain the transport parameters of this theoretical approach in Sec. IV A, the analytical approximation of the Soret coefficient will be fitted to the experimentally detected development of the Soret coefficient which is calculated via (3).

The fluid's characterisation in Sec. II and the description of the experimental setup in Sec. III A lead to the experimental separation curves in Sec. III B. First the Soret coefficient is calculated via a fit of the measured data to the linear Eq. (3) in this section. The data are then additionally analysed analytically in Sec. IV A and numerically in Sec. IV B. The analytical investigation determines the development of the magnetic Soret coefficient with the magnetic field applied by fitting the analytical expression¹⁶ of the Soret coefficient to the one obtained by the measurement and Eq. (3). The results are the thermodynamical parameters ξ_{\parallel} and ξ_{\perp} . The numerical investigation fits the separation curve numerically obtained from Eq. (8) to the measured data. The results again are the transport parameters. The Soret coefficient in this numerical case can only be determined via the transport parameters and either the analytical approximation of the Soret coefficient or the linear approximation in Eq. (3).

II. FLUID CHARACTERISATION

The fluid under investigation is the EMG905-fluid prepared by Ferrotec. For the purpose of analysing thermodiffusive processes several physical parameters of this particular magnetic fluid have to be determined, such as the particle size distribution and the average particle diameter d , the volume concentration of magnetic particles, the dynamic viscosity, the diffusivity of the particles and the pyromagnetic coefficient, describing the change in magnetisation with change in temperature of the fluid. Since the thermodiffusive behaviour of the EMG905-fluid has already been investigated for vanishing magnetic fields, these parameters and their determination, described in detail in a previous work,³ will be used here.

The volume concentration and the average particle diameter have been determined to $\varphi = 0.0867$ and $d = 10.4$ nm via the experimentally determined magnetisation curve fitted by²⁰

$$M = M_d \varphi \left[\coth(\alpha) - \frac{1}{\alpha} \right]. \quad (9)$$

The particles' average diameter is calculated by processing the magnetisation curve with the Chantrell method.²² The experimental curve is thereby fitted by Eq. (9), based on the Langevin-description, extended to a more realistic lognormal distribution of the particles' size. The particles of the EMG905-fluid consist of magnetite with a density of $\rho_P = 5150$ kg/m³, the fluid's density ρ is approximated to $\rho = 1000$ kg/m³. With these values the mass concentration c reads $c = \frac{\rho_P}{\rho} \varphi = 0.447$. The dynamic viscosity, since it is not affected by the magnetic field in the case of the EMG905-fluid,²⁴ is determined to $\eta = 0.011$ Pa s at 298 K.^{3,11} The dependency of the diffusion coefficient, being $D = 3.92 \times 10^{-12}$ m²/s in the non-magnetic case,^{3,11} on the magnetic field, can be investigated based on different theoretical models,^{8,9,23,25,26} from which the theoretical description of Morozov²³ for concentrated ferrofluids was adapted to the present fluid parameters.

The theoretical model of Morozov²³ assumes hydrodynamic dipole-dipole-interaction between the particles and also considers the influence of the magnetic energy in the system on the transport process. The anisotropic behaviour of the diffusion coefficient is expressed by regarding the relative change in the diffusion coefficient with increasing magnetic field strength. Morozov²³ describes the change in diffusivity with the magnetic field being aligned parallel via

$$\frac{\Delta D_{\parallel}}{D} = \frac{D_{\parallel} - D}{D} = \frac{\mu_0}{k_B T \tilde{\omega}} (1 + \chi^{-1} - \chi_i^{-1}) M(H)^2 \frac{V}{\varphi} \quad (10)$$

or being aligned perpendicular to the diffusion direction by

$$\frac{\Delta D_{\perp}}{D} = \frac{D_{\perp} - D}{D} = \frac{\mu_0}{k_B T \tilde{\omega}} (\chi^{-1} - \chi_i^{-1}) M(H)^2 \frac{V}{\varphi}. \quad (11)$$

D denotes the diffusion coefficient for vanishing magnetic fields, $\tilde{\omega}$ denotes the so called "inverse compressibility" and is experimentally determined²³ to $\tilde{\omega} = 1 + 20\varphi$. The experimentally determined initial susceptibility χ is measured to 1.468 by the magnetisation curve. The theoretical initial susceptibility $\chi_i = \frac{\pi \varphi \mu_0 M_d^2 d^3}{18 k_B T}$ by Rosensweig²⁰ is determined to 1.052 with $M_d = 450$ kA/m. The average temperature which is applied to the fluid in the thermodiffusion experiments is $T = 298$ K.

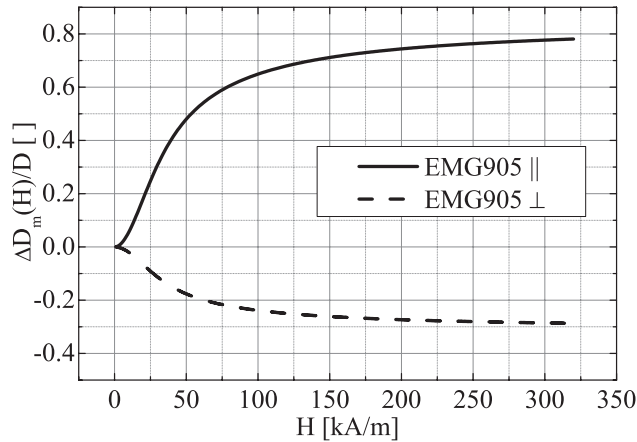


FIG. 1. The magnetic field dependent behaviour of the relative change in the diffusion coefficient based on a theoretical approach of Morozov²³ shows an anisotropic development. A magnetic field aligned parallel with the diffusion direction enhances, a perpendicular position hinders the diffusivity of the EMG905-ferrofluid.

The anisotropic development of the diffusion coefficient in Figure 1 points out that a magnetic field being aligned parallel to the diffusion direction enhances diffusivity, i.e., with rising magnetisation of the fluid the value of the diffusion coefficient rises as well. The opposite behaviour is found for a perpendicular positioning. The diffusivity decreases with rising magnetic field strengths, the diffusion coefficient is then smaller than the one for vanishing magnetic fields.

The pyromagnetic coefficient

$$K = \left. \frac{\partial M}{\partial T} \right|_{H=const} \quad (12)$$

describes the temperature dependency of the magnetisation and can be calculated by detecting magnetisation curves at different temperatures at constant magnetic field strengths. The result for the pyromagnetic coefficient calculated via this procedure is shown in Figure 2 for the EMG905-ferrofluid. For small magnetic field strengths the coefficient rises linearly with the applied magnetic field until reaching a maximal value of about $K = 60$ A/mK at a field strength around $H = 80$ kA/m. For field strengths above that value the coefficient saturates at approximately $K = 52$ A/mK.

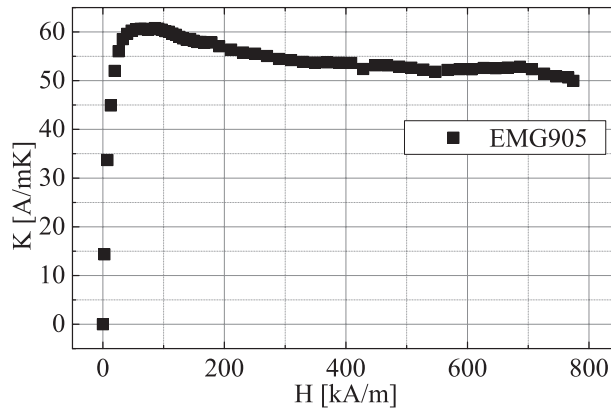


FIG. 2. The pyromagnetic coefficient K describes the change in magnetisation induced by a change in the fluid's temperature. The data are calculated via 5 magnetisation curves from 288 K to 308 K with equally distanced temperatures for the EMG905-ferrofluid. For small magnetic field strengths K depends linearly on H and saturates for high magnetic field strengths.

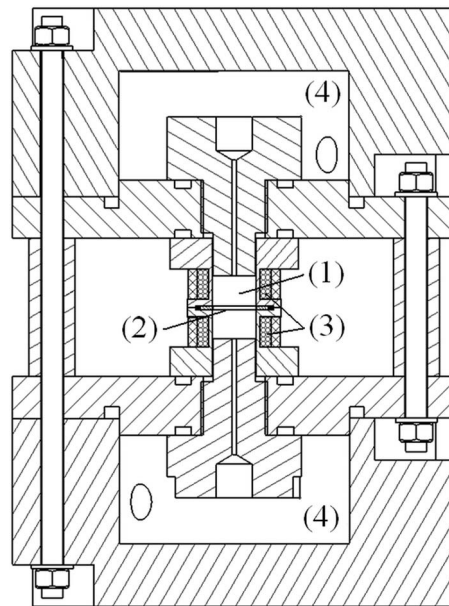


FIG. 3. Main components of the horizontal thermodiffusion cell:⁴ (1) fluid container for the EMG905-fluid ($h = 14$ mm), (2) double-layer grid ($h_g = 1.5$ mm), which bounds the separation area, (3) sensor coils, detecting the fluid's concentration in the fluid reservoirs, and (4) tempering water baths for the application of the temperature gradient. Reprinted with permission from L. Sprenger, A. Lange, and S. Odenbach, "Thermodiffusion in concentrated ferrofluids - A review and current experimental and numerical results on non-magnetic thermodiffusion," *Phys. Fluids* **25**, 122002 (2013); L. Sprenger, A. Lange, and S. Odenbach, "Thermodiffusion in ferrofluids regarding thermomagnetic convection," *C. R. Mec.* **341**, 429–437 (2013). Copyright 2013 Académie des sciences/Elsevier Masson SAS.^{3,11}

III. EXPERIMENTAL INVESTIGATION ON THERMODIFFUSION

A. Experimental setup

For the determination of the magnetic thermal diffusion in ferrofluids a horizontal thermodiffusion cell based on a design taken from the work of Völker and Odenbach⁴ is used as can be seen in Figure 3.¹¹ The fluid container (1) with a height of $h = 14$ mm is placed in the centre and consists of the separation area between the double-layer grid (2) with a height of $h_g = 1.5$ mm and the two fluid reservoirs above and below the grid, while the temperature gradient is applied via the water baths (4). The sensor coils (3), wrapped around the container, sample the average concentration in each fluid reservoir. A detailed characterisation of the thermodiffusion cell and the proof for its applicability in a non-magnetic environment can be found in other works of the authors.^{3,27} For the application of the setup within a magnetic field two further issues have to be considered. This is on the one hand the influence of the grid material on the magnetic separation process and on the other hand the influence of the magnetic field applied during the experiment on the sampling of the sensor coils' inductances.

As in a non-magnetic experimental setup the double-layer grid, being positioned within the diffusion flow of the magnetic fluid, has to be tested for any influence on the diffusion process. In the present case the relative permeability of the grid material being different from the permeability of the fluid could possibly induce perturbances and lead to microconvection within the separation area between the two grids²⁸ resulting in a separation signal not only due to thermodiffusion. Figure 4 shows the relative concentration difference between the lower and upper fluid reservoir when exposing the fluid to a temperature gradient of 1 K/mm. In the case of no magnetic field applied as well as in the case of the field being aligned parallel with the temperature gradient with a strength of $H = 320$ kA/m the slope of the separation signal is not significantly dependent on the grid material used. Therefore, microconvective contributions to the thermodiffusive measurement signal can be excluded.

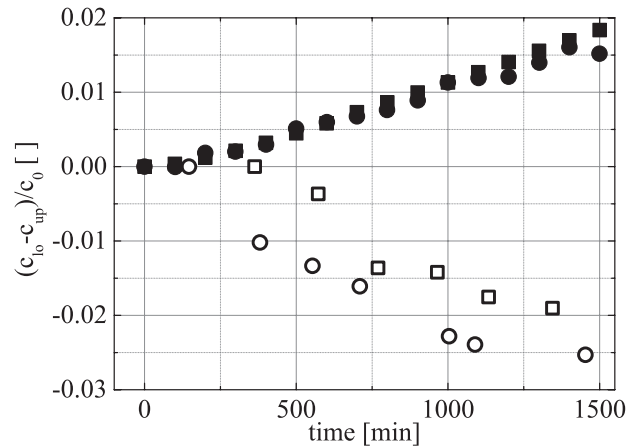


FIG. 4. Development of the relative concentration difference between lower and upper fluid reservoir of the measuring cell in time and either with (\square , \circ) or without (\blacksquare , \bullet) a magnetic field of $H = 320$ kA/m applied parallel to the temperature gradient of 1 K/mm. Brass (\blacksquare , \square) or a polyamide (\bullet , \circ) is used as grid material.

It also has to be ensured that the measurement signal of the sensor coils only shows the change in concentration due to thermodiffusion and not any influence of the magnetic field on the coils' inductances. For that purpose a first measurement of the inductance of the lower sensor coil is carried out at $H = 340$ kA/m but at a homogeneous temperature in the fluid cell filled with the EMG905-fluid. Separation will not take place and therefore a constant inductance is expected in such a setup. Figure 5 shows the development of the mentioned inductance with time. The coil's inductance rises for the first 500 min of measurement by $0.6 \mu\text{H}$ and then oscillates around an approximately constant value with $\pm 0.1 \mu\text{H}$. The change in inductance during a separation experiment is expected to be around $1 \mu\text{H}$ and is therefore considerably larger than these oscillations. A further consequence is the first 3 to 4 sampled data points in the following experiments have to be either neglected or evaluated thoroughly in each specific case. While in this prerequisite experiment the fluid cell is filled with the EMG905-fluid, the influence of the remanence magnetic field on the inductance of the sensor coils is tested in a second experiment applying the field to an empty fluid cell. The temperature is kept constant at the fluid container, the magnetic field strength is set to $H = 340$ kA/m. Within a day and an equal distance of time of 3 h the magnetic field is shut off for approximately 10 min and then switched on again. Figure 6, showing the inductance over time and marking the off-time by

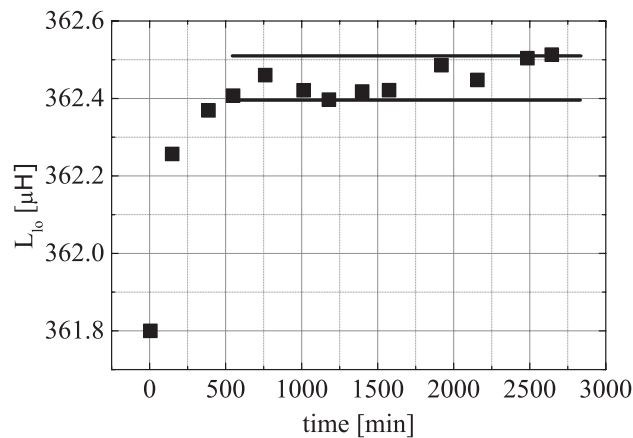


FIG. 5. Development of the inductance of the lower sensor coil of the filled fluid container of the thermodiffusion cell at a constant fluid temperature. The magnetic field strength is adjusted to $H = 340$ kA/m, the black solid lines mark the boundary values of the inductance's oscillation.

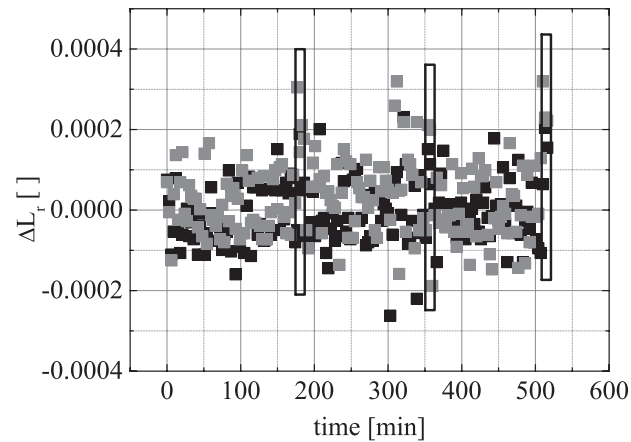


FIG. 6. Development of the relative inductances of the upper (■) and lower (■) sensor coil in an empty fluid container at a constant temperature and a magnetic field strength of 340 kA/m. The magnetic field is switched off and on regularly, the black rectangles mark the shut-off time of the field of 10 min.

the black rectangles, points out that the coils' inductances do not change in a significant way due to the measurement procedure. Figure 7 visualises the field strength during the on-time (□) and the off-time (■) over the entire thermodiffusion cell. The position of the fluid container, placed in the centre of the two pole shoes is explicitly marked by the grey rectangle and the container's sketch. Even though the parallel measured remanence field strength is about 1.5 kA/m it does not have a significant influence on the inductance signal of the coils, as shown in Figure 6.

These preliminary investigations prove that the horizontal thermodiffusion cell as pictured in Figure 3 besides leading to appropriate measurement data in non-magnetic experiments,³ can also be reliably used for the detection of the magnetic separation process.

B. Separation experiments

The separation experiments on the EMG905-fluid are carried out with either a parallel or a perpendicular alignment of the magnetic field with the temperature gradient of 1 K/mm applied to the fluid layer. The magnetic field strength is chosen among $H = 40$ kA/m, $H = 100$ kA/m, and $H = 320$ kA/m. The general procedure of the separation detection is described in detail in a

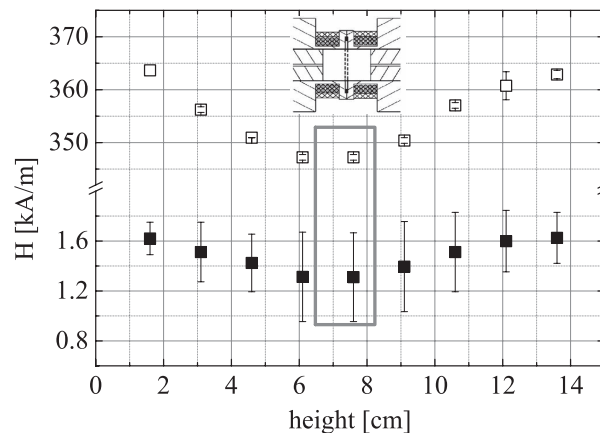


FIG. 7. Development of the applied magnetic field H (□) and the remanence field strength H_R (■) after shutting the field off over the thermodiffusion cell, the grey rectangle marks the position of the fluid container.

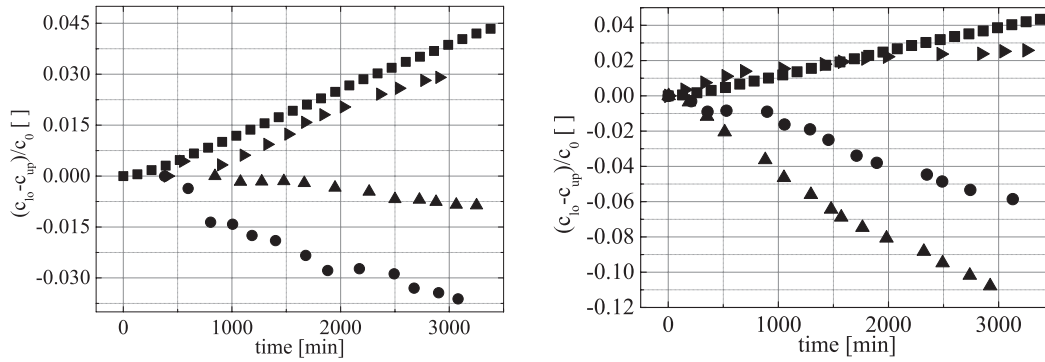


FIG. 8. Experimental separation curves for $H = 0$ kA/m (■), $H = 40$ kA/m (►), $H = 100$ kA/m (▲), and $H = 320$ kA/m (●) and a temperature gradient of 1 K/mm. The magnetic field is positioned parallel on the left-hand side and perpendicular on the right-hand side to the thermal gradient. Small magnetic fields lead to a positive but weakened slope of the separation signal in comparison with the non-magnetic case, larger fields lead to negative slopes indicating a change in the particles' direction of movement. Reprinted with permission from L. Sprenger, A. Lange, and S. Odenbach, "Thermomagnetic convection in ferrofluids regarding thermomagnetic convection," *C. R. Mec.* **341**, 429–437 (2013); L. Sprenger, A. Lange, and S. Odenbach, "Influence of thermomagnetic convection on thermomagnetic convection in magnetic fluids," *Magneto hydrodynamics* **49**, 473–478 (2013). Copyright 2013 Académie des sciences/Elsevier Masson SAS.^{11,27}

previous work¹¹ and is mentioned here briefly. Directly linked with the detection of the change in concentration is the calibration of the inductance signal. Therefore, the measurement cycle starts with the sampling of the inductances of the sensor coils when the fluid cell is empty, no magnetic field is applied but the temperature gradient is. The inductances are registered until they reach a stationary stage representing the inductance at a particle volume concentration of $\varphi = 0$ vol. %. Then the cell is filled with the EMG905-fluid and exposed to the average temperature of $T = 298$ K used afterwards in the experiment. When again a stationary value is reached the temperature gradient is applied and the magnetic field is switched on after 10 min. The average inductance signal of the first 10 min, with the concentration being $\varphi = 8.67$ vol. %, is used to be compared with the inductance for $\varphi = 0$ vol. % to calibrate the measurement system. In the following process the magnetic field is switched off every 3 h to detect the inductance of the filled cell during a time of about 10 min. Figure 8 on the left-hand side shows the development of the relative concentration difference over time due to the magnetic field applied. For a small field strength of $H = 40$ kA/m the slope of the curve is positive indicating a positive Soret coefficient of $S_{T\parallel} = 0.12$ K⁻¹ via Eq. (3). Rising magnetic field strengths then lead to a change in the direction of the particles' movement indicated by a negative slope of the separation curve. The coefficient can be calculated to $S_{T\parallel} = -0.037$ K⁻¹ ($H = 100$ kA/m) and $S_{T\parallel} = -0.085$ K⁻¹ ($H = 320$ kA/m) using Eq. (3). The diffusion coefficient is considered in its magnetic field dependent form by $D_{\parallel} = \{5.52; 6.46; 6.97\} \times 10^{-12}$ m²/s for the three strengths of the magnetic field.

The case of the perpendicular positioned magnetic field is presented in Figure 8 on the right-hand side showing a similar behaviour as in the parallel setup. Small magnetic fields weaken the separation process resulting in a decrease in the slope of the magnetic separation in comparison to the one in the non-magnetic separation. But with rising field strengths the direction of the moving particles is reversed and becomes stronger, indicated by a negative slope increasing with the rising field strength. An analysis of the separation data with Eq. (3) and the magnetic diffusion coefficient for the perpendicular case $D_{\perp} = \{3.33; 2.98; 2.78\} \times 10^{-12}$ m²/s leads to the corresponding magnetic Soret coefficient $S_{T\perp} = \{0.099; -0.673; -0.36\}$ K⁻¹ for the three non-zero values of the magnetic field strength.

These experimental results are used in the following to validate the theoretical approaches. Therefore, two different points of view are considered. First, an analytical description of the Soret coefficient is used to fit the experimentally calculated coefficients in Sec. IV A. Second, a numerical calculation of the separation curves is compared to the experimental ones in Sec. IV B.

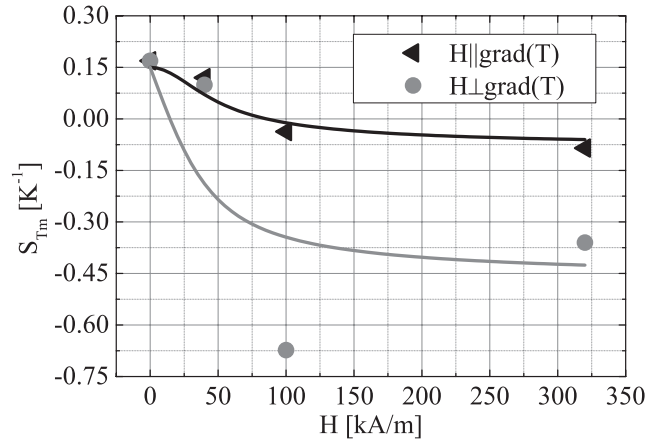


FIG. 9. The experimental magnetic Soret coefficient, parallel (\blacktriangleleft) and perpendicular (\bullet), including a magnetic diffusion coefficient is compared with an analytical approximation of the coefficient, parallel ($-$) and perpendicular ($-$), based on the FFD-theory.¹⁶ The relevant transport coefficients can be determined to $\xi_{\parallel} = 7.5 \times 10^{-22} \text{ kg}/(\text{A}^2\text{m})$ and $\xi_{\perp} = -6 \times 10^{-4} \cdot \frac{D_{\perp}}{C} \text{ kg}/(\text{Am}^2)$ and show a good agreement with the qualitative development of the coefficient with rising magnetic field strength.

IV. THEORETICAL INVESTIGATION ON THERMODIFFUSION AND COMPARISON WITH EXPERIMENTAL RESULTS

A. Analytical investigation

As mentioned in the Introduction an analytical approximation for the magnetic Soret coefficient is provided by Lange¹⁶ for the two orientations of the magnetic field. It is derived from the thermodynamical approach of the concentration profile in the fluid container according to the diffusive mass flux of Eq. (8). Assuming that the transport coefficients ξ and ξ_1 , as being necessary for the analytical description, can be determined from the non-magnetic separation process³ leads to a rough fit of the analytical Soret coefficient with the experimental one via ξ_{\parallel} in the parallel and via ξ_{\perp} in the perpendicular field orientation. Figure 9 shows the plot of the Soret coefficient calculated by the experimentally detected separation curves analysed with the theoretical equation of Lange¹⁶ and considering the magnetic diffusion coefficient (symbols), as well as the analytically determined development of the coefficient by rising magnetic field strengths (solid lines). This analytical approach is qualitatively able to represent the dependency of the coefficient on the field strength. For both field orientations adequate transport parameters can be fitted: $\xi_{\parallel} = 7.5 \times 10^{-22} \text{ kg}/(\text{A}^2\text{m})$ and $\xi_{\perp} = -6 \times 10^{-4} \cdot \frac{D_{\perp}}{C} \text{ kg}/(\text{Am}^2)$. This fit assumes that the two non-magnetic parameters ξ and ξ_1 are based on $m_1 = 1.489 \times 10^{-25} \text{ kg}$ and $m_2 = 2.474 \times 10^{-25} \text{ kg}$, being the mass of one molecule of the solid (1) and liquid (2) phase. The determination of these values is based on two restrictions. The first is the fit of the analytical Soret coefficient with the experimental data. It is only possible for masses being in the same order of magnitude. The second is then the approximate molecular mass of magnetite and the fluid's carrier liquid. Both thoughts point at a general restriction of the FFD, which should be investigated in more detail in further works. Here, the values of m_1 and m_2 then lead to $\xi = 1.927 \times 10^{-13} \text{ kg}/\text{m}^3$, and $\xi_1 = 3.033 \times 10^{-10} \text{ kg}/(\text{ms K})$.

The measured data are compared with former experimental results from Völker and Odenbach⁴ (grey triangle (\blacktriangleleft), grey bullet (\bullet)) in Figure 10 who investigated a dilute ferrofluid of $\varphi = 0.02$ with a low viscous carrier liquid. The diffusivity of this fluid is one order of magnitude higher than the presently analysed fluid and the non-magnetic diffusion coefficient had been determined to $D = 2 \times 10^{-11} \text{ m}^2/\text{s}$. The qualitative development of the Soret coefficient with the magnetic field strength with a parallel orientation of the magnetic field is similar for both tested fluids: A small field strength leads to a weaker separation in comparison to the non-magnetic case, larger field strengths turn the particles' flux direction and then strengthen it. Taking a look at the perpendicular orientation of the magnetic field reveals that the behaviour of the two fluids investigated shows a contrary development. While the present fluid also, as already mentioned, leads to a change in the

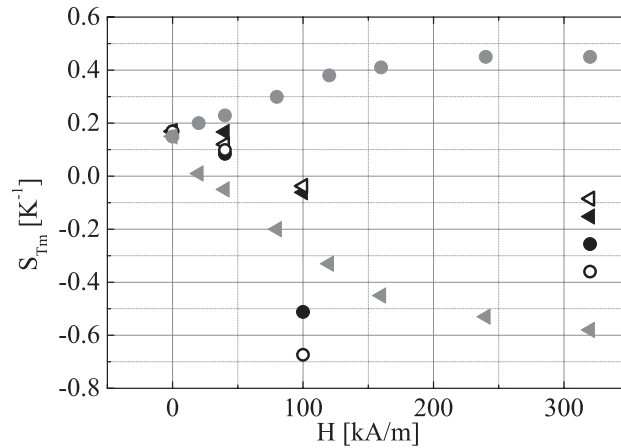


FIG. 10. Experimentally detected magnetic Soret coefficients for the two field orientations parallel (\blacktriangleleft , \blacktriangle , \blacktriangleleft) and perpendicular (\circ , \bullet , \bullet) to the temperature gradient (\blacktriangleleft , \blacktriangle , \circ , \bullet) in comparison with former data with a different ferrofluid (\blacktriangleleft , \bullet).⁴ The current data are on the one hand calculated with the constant non-magnetic diffusion coefficient, parallel (\blacktriangleleft) and perpendicular (\bullet), and on the other hand by considering the magnetic field dependency of the diffusion coefficient $D_m = D_m(H)$, parallel (\triangleleft) and perpendicular (\circ).

particles' flux direction due to the magnetic effects, the former experiments do not show such a behaviour. The separation process is merely strengthened by the magnetic field and saturates for high field strengths. Therefore, it can be assumed that the separation behaviour of magnetic fluids is not independent of the concentration of the fluid, i.e., it is probably a rather specific property of each tested fluid.

With the differing behaviour between the two differently concentrated fluids, the question is whether the former measurement data can still be fitted with the analytical Soret coefficient used here. Figure 11 presents a fit for the former experimental coefficient with the same procedure as for the current data. The transport coefficient ξ is determined with the non-magnetic diffusion equation to $\xi = 0.0806 \cdot D \text{ kg/m}^3$, which differs from the analysis in Ref. 16. The magnetic data fit then leads to $\xi_{\parallel} = 1 \times 10^{-9} \cdot D_{\parallel} \text{ kg/(A}^2\text{m)}$ in the parallel, and $\xi_{\perp} = 2.7 \times 10^{-4} \cdot \frac{D_{\perp}}{c} \text{ kg/(Am}^2\text{)}$ in the perpendicular case. Also in this experimental case the FFD-theory, applied to the currently investigated fluids, makes it possible to find a consistent set of parameters representing the experimentally determined

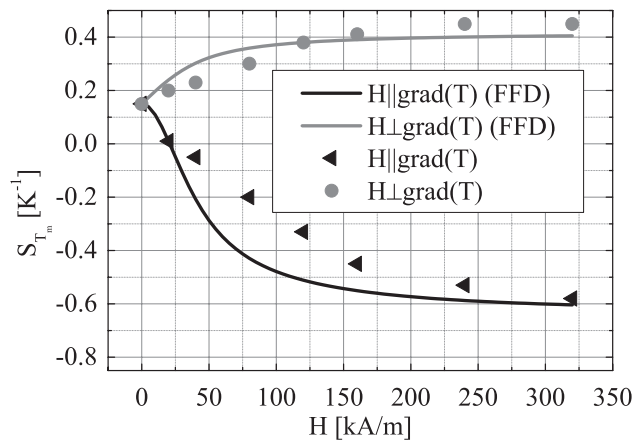


FIG. 11. The experimentally obtained magnetic Soret coefficient in former measurements,⁴ with parallel (\blacktriangleleft) and perpendicular (\bullet) orientation of the magnetic field, is compared with an analytical fit, parallel ($-$) and perpendicular ($-$), for the coefficient's development with the field strength, proving that an adequate fit can also be obtained for this data of a dilute magnetic fluid with $\xi = 0.0806 \cdot D \text{ kg/m}^3$, $\xi_{\parallel} = 1 \times 10^{-9} \cdot D_{\parallel} \text{ kg/(A}^2\text{m)}$, and $\xi_{\perp} = 2.7 \times 10^{-4} \cdot \frac{D_{\perp}}{c} \text{ kg/(Am}^2\text{)}$.

Soret coefficient. Even though the magnetic Soret coefficient for the two different sets of measured data is qualitatively different in the case that the magnetic field is positioned perpendicular to the temperature gradient, both cases can be fitted with the analytical solution based on the work of Lange.¹⁶

All these results are based on the determination of the Soret coefficient by Eq. (3), which assumes a dilute magnetic fluid being investigated, which is a weakness of the theory while analysing concentrated fluids as in the present case. The numerical calculation of the concentration distribution in the fluid container does not assume a dilute fluid being analysed, and is employed as a different approach to reproduce the measured signal.

B. Numerical investigation

The numerical analysis starts with the case of the magnetic field being positioned parallel to the temperature gradient. Combining Eq. (8) and $\frac{\partial c}{\partial t} = -\frac{\vec{\nabla} \cdot \vec{j}}{\rho}$ for such an alignment leads to a diffusion equation containing spatial derivatives in one dimension,

$$\frac{\partial c_{1\parallel}}{\partial t} = (\xi + \xi_{\parallel} M^2) \left[\frac{\partial \tilde{\mu}_c}{\partial \rho} + \frac{\mu_0}{\rho} \frac{\rho}{\rho_P} \left(\frac{\partial M}{\partial \rho} \right)^2 \right] \frac{\partial^2 c}{\partial z^2}. \quad (13)$$

The boundary condition requires no mass flux over the cell's wall by $j_z = 0$ and the initial condition is set to $c(t = 0) = c_0$ with c_0 denoting the homogeneous mass concentration of the fluid.

If the magnetic field is aligned perpendicular to the temperature gradient the resulting diffusion equation being the starting point of numerical investigation contains now spatial derivatives in three dimensions

$$\frac{\partial c_{1\perp}}{\partial t} = \frac{\partial \tilde{\mu}_c}{\partial \rho_1} \left[(\xi + \xi_{\parallel} M^2) \frac{\partial^2 c}{\partial x^2} + \xi \left(\frac{\partial^2 c}{\partial y^2} + \frac{\partial^2 c}{\partial z^2} \right) \right] \quad (14)$$

in contrast to Eq. (13). The boundary conditions as in the parallel case read

$$j_x = 0 = (\xi + \xi_{\parallel} M^2) \frac{\partial c}{\partial x}, \quad (15)$$

$$j_y = 0 = -\frac{\partial \tilde{\mu}_c}{\partial T} \frac{\xi_{\perp}}{\rho} \frac{\partial T}{\partial z} M + \frac{\partial \tilde{\mu}_c}{\partial \rho_1} \left(\xi \frac{\partial c}{\partial y} - \xi_{\perp} M \frac{\partial c}{\partial z} \right), \quad (16)$$

$$j_z = 0 = \left(\frac{\xi_1}{\rho} + \frac{\xi}{\rho} \frac{\partial \tilde{\mu}_c}{\partial T} \right) \frac{\partial T}{\partial z} + \frac{\partial \tilde{\mu}_c}{\partial \rho_1} \left(\xi \frac{\partial c}{\partial y} + \xi_{\perp} M \frac{\partial c}{\partial z} \right), \quad (17)$$

and assume that the boundaries are impermeable. The initial condition again requires that the fluid's mass concentration is homogeneous with c_0 when $t = 0$.

The numerical method used here to solve both diffusion equations is the finite differences method (FDM). Spatial derivatives are calculated with the central differences scheme, while the boundary conditions are implemented either by the backwards scheme for the upper boundary or the forward scheme for the lower boundary. The time derivative is considered by the Euler backwards scheme.²⁹⁻³¹ The result of the numerical calculation is the concentration profile of the fluid under the effect of magnetic field and temperature gradient in the fluid container of the height $h = 14$ mm. To realise the comparison with the experimental separation curve, the concentration is averaged over each fluid reservoir's height and the relative concentration difference can be determined with these average values.

Figure 12 shows the result of the fit in the case of the parallel orientation of the magnetic field with the temperature gradient. If the transport parameters are determined to $\xi = 1.927 \times 10^{-13}$ kg/m³ and $\xi_1 = 3.033 \times 10^{-10}$ kg/(ms K) in the non-magnetic case, the magnetic parameter can be fitted to $\xi_{\parallel} = \{2.8; 9.1; 11.2\} \times 10^{-11} \cdot D_{\parallel}$ kg/(A²m), which leads to a very good agreement with the experimental data. But, as is emphasised in Figure 13, the magnetic coefficient varies with the magnetic field strength.

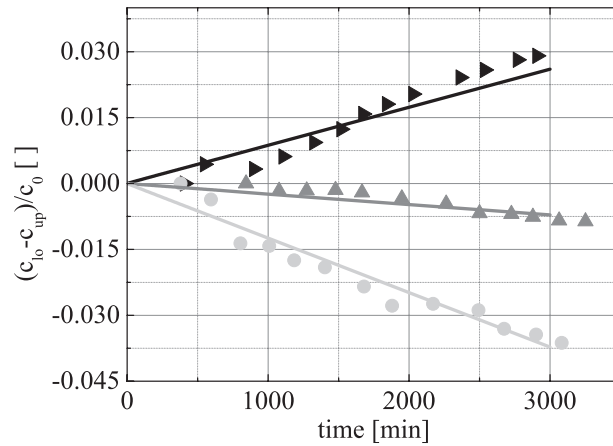


FIG. 12. Experimental separation curves with $H = 40$ kA/m (\blacktriangleright), $H = 100$ kA/m (\blacktriangle), and $H = 320$ kA/m (\bullet) and $\vec{H} \parallel \vec{\nabla}(T)$ compared with the separation development numerically detected via the FFD-theory (solid lines). The transport coefficient is determined to $\xi_{\parallel} = \{2.8; 9.1; 11.2\} \times 10^{-11} \cdot D_{\parallel}$ kg/(A²m) and leads to a good agreement between experimental and numerical result.

The determination of the Soret coefficient is then again based on either Eq. (3), which still does not account for concentrated magnetic fluids, or on an analytical approach, considering the determined transport parameter ξ_{\parallel} , $S_{T\parallel} = \{0.11; -0.041; -0.079\} \text{ K}^{-1}$. Figure 14 presents the experimental separation curves for the perpendicular orientation of the magnetic field and the field strengths $H = 40$ kA/m, 100 kA/m, and 320 kA/m. The numerical calculation fitting the curve of the smallest field strength leads to $\xi_{\perp} = 1 \times 10^{-17} \text{ kg}/(\text{Am}^2)$. Using the same value for the other field strengths does not show the expected weakening of the separation, but a rise in the process's intensity with the field strength. To take a closer look at the dependency of the separation curves on ξ_{\perp} , different values for the parameter are used to calculate the separation, which is shown in Figure 15 (left side). Larger values for ξ_{\perp} than used in Figure 14 increase the intensity of the separation, but still with a rising positive slope of the separation curve for rising magnetic field strength. For smaller values the separation is no longer dependent on the different field strengths. Using a negative transport coefficient as shown in Figure 15 (right side) does not have an impact on the separation. The calculated data for the two parameters are identical.

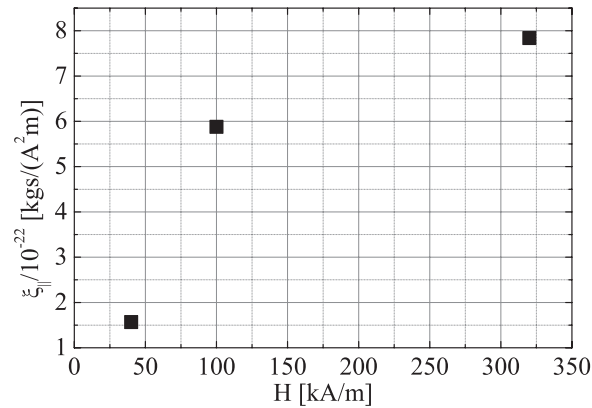


FIG. 13. Development of the transport coefficient ξ_{\parallel} with the magnetic field strength $H = \{40; 100; 320\}$ kA/m applied to the separation cell. The initial assumption of the introductory part, considering the coefficient as a constant value does not hold for the fitting of the experimental and numerical separation signal.

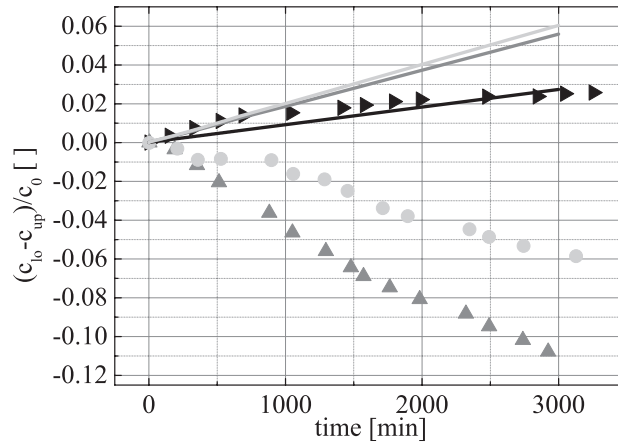


FIG. 14. Experimental separation curves with $H = 40$ kA/m (\blacktriangleright), $H = 100$ kA/m (\blacktriangle), and $H = 320$ kA/m (\bullet) and $\vec{H} \perp \vec{\nabla}(T)$ compared with the separation development numerically detected via the FFD-theory (solid lines). The transport coefficient is determined to $\xi_{\perp} = 1 \times 10^{-17}$ kg/(Am²) and leads to a good agreement between experimental and numerical result for $H = 40$ kA/m. A fitting for the other field strengths could not be found.

For the perpendicular case it is therefore not possible to find a consistent numerical simulation for the concentration development being similar to the one observed in the experiments. No Soret coefficient different from the experimentally and analytically calculated one can be determined.

While an agreement between theory and experiment can be found for a magnetic field position parallel to the temperature gradient analytically as well as numerically, this is not the case in the perpendicular setup. Analytically, it is possible to find a fitting parameter for the Soret coefficient, but numerically, finding a fitting parameter for the separation curve could not be concluded. The comparison with former data of Völker and Odenbach⁴ carried out with a magnetic fluid being different from the EMG905-fluid suggests that the difference of the fluids especially in concentration and diffusivity leads to a significantly different magnetic separation behaviour.

V. RESULTS AND DISCUSSION

Since thermodiffusion depends on the composition of the fluid under investigation and thereby for a great part on its magnetic properties and diffusivity, the determination of the pyromagnetic

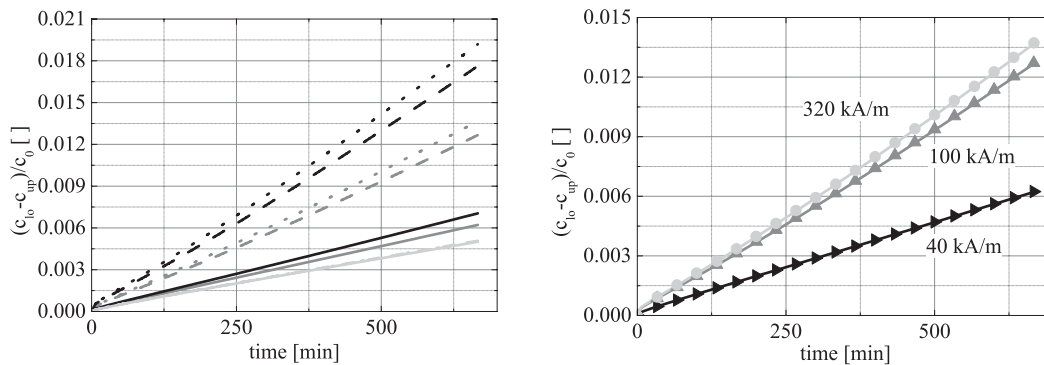


FIG. 15. Numerically determined separation signal for different field strengths using different values for the transport coefficient ξ_{\perp} . In the left figure $\xi_{\perp} = 1.3 \times 10^{-17}$ kg/(Am²) (black solid line), $\xi_{\perp} = 1 \times 10^{-17}$ kg/(Am²) (grey solid line), and $\xi_{\perp} = 1 \times 10^{-18}$ kg/(Am²) (light grey solid line) with $H = 40$ kA/m (\rightarrow), 100 kA/m ($- -$), and 320 kA/m (\cdots) are applied. In the right figure $\xi_{\perp} = 1 \times 10^{-17}$ kg/(Am²) (black solid line, grey solid line, and light grey solid line) and $\xi_{\perp} = -1 \times 10^{-17}$ kg/(Am²) (\blacktriangleright , \blacktriangle , \bullet) with $H = 40$ kA/m (\rightarrow), 100 kA/m ($-$), and 320 kA/m (\leftarrow) are applied. No value can be determined which leads to a change in the separation direction of the fluid.

TABLE I. Fluidparameters of the EMG905-fluid either obtained by the experimental separation with or without a magnetic field applied or theoretical investigations.

		0 kA/m	40 kA/m	100 kA/m	320 kA/m
$S_{T\parallel} (D)$	K^{-1}	0.169	0.167	-0.061	-0.152
$S_{T\perp} (D)$	K^{-1}	0.169	0.084	-0.512	-0.257
$S_{T\parallel} (D_{\parallel})$	K^{-1}	0.169	0.12	-0.037	-0.085
$S_{T\perp} (D_{\perp})$	K^{-1}	0.169	0.099	-0.673	-0.36
D_{\parallel}	m^2/s	3.92×10^{-12}	5.52×10^{-12}	6.64×10^{-12}	6.97×10^{-12}
D_{\perp}	m^2/s	3.92×10^{-12}	3.33×10^{-12}	2.98×10^{-12}	2.78×10^{-12}
ξ_{\parallel}	$kg/(A^2m)$		$2.8 \times 10^{-11} \cdot D_{\parallel}$	$9.1 \times 10^{-11} \cdot D_{\parallel}$	$11.2 \times 10^{-11} \cdot D_{\parallel}$
ξ_{\perp}	$kg/(Am^2)$		1×10^{-17}	1×10^{-17}	1×10^{-17}

coefficient and the magnetic diffusion coefficient as requirement for the analysis of the magnetic separation curves was focused on. Among the different approaches^{9,19,23,26,32,33} the theory for concentrated magnetic fluids by Morozov²³ applies best and leads to the expected anisotropy in diffusivity. Diffusion is enhanced by a magnetic field aligned parallel with the temperature gradient, while the perpendicular positioned field leads to a hindrance in diffusion. For the field strengths $H = 40$ kA/m, 100 kA/m, and 320 kA/m the coefficient is determined to $D_{\parallel} = 5.52 \times 10^{-12}$ m²/s, 6.46×10^{-12} m²/s, and 6.97×10^{-12} m²/s in the parallel and in the perpendicular case to $D_{\perp} = 3.33 \times 10^{-12}$ m²/s, 2.98×10^{-12} m²/s, and 2.78×10^{-12} m²/s, these values are summed up in Table I. Measuring the coefficient experimentally for a magnetic field applied as well as for vanishing magnetic fields is still an open topic to be accomplished.

The qualitative behaviour of the magnetic thermodiffusion measured with the concentrated EMG905-ferrofluid is characterised by two main features. First, a weakening of thermal transport for small magnetic field strengths and nanoparticles moving to the cold part of the cell, which corresponds to a positive Soret coefficient, second, a change in the particles' direction of movement with a further rising field strength. The strength of both features is independent of the alignment of the field. Contrary, the intensity of the separation of particles and carrier liquid is anisotropic and stronger in the perpendicular alignment, the specific values of the parallel and perpendicular Soret coefficient can be found in Table I. It is further distinguished if a constant or field-dependent diffusion coefficient is used to calculate the Soret coefficient. The values of these, as shown in Table I, are of course different from each other, but the change in the particles' direction remains the same. For a constant diffusion coefficient of $D = 3.92 \times 10^{-12}$ m²/s the Soret coefficients can be calculated to: $S_{T\parallel} = 0.167$ K⁻¹, -0.061 K⁻¹, and -0.152 K⁻¹, $S_{T\perp} = 0.084$ K⁻¹, -0.512 K⁻¹, and -0.257 K⁻¹.

Comparing these experimental results with former measurements on the magnetic Soret-effect in a different magnetic fluid, an agreement in the results can be found for the parallel alignment. The perpendicular magnetic field in former experiments did not provoke a change in the direction of the moving particles. Therefore, the Soret-effect must be considered fluid-specific.

The numerical investigation of thermodiffusion on the basis of the diffusive mass flux described by the FFD-theory via two independent parameters ξ_{\parallel} and ξ_{\perp} is capable of calculating separation curves which can be fitted to the experimental ones in the case of a parallel alignment of magnetic field and temperature gradient, see Table I. The fit is not entirely possible for the perpendicular case. For the perpendicular alignment only positive slopes for the separation are determinable independent of magnitude and sign of the transport coefficient. Both fits are sensitive to the definition of the fluid's components' masses entering the FFD-theory which is a weakness of the approach that has to be considered and investigated in more detail on a broader base of experimental data.

The magnetic Soret coefficient as shown in the different experimental, analytical, and numerical investigations of the present work is a fluid-specific value which reacts to different compositions of the fluid such as concentration, carrier liquid and the diffusive properties. It is neither possible to predict a value for the coefficient in the magnetic application nor the anisotropic behaviour. Broader studies on different fluids containing different amounts of nanoparticles may help to achieve a more

detailed idea of the parameters mainly influencing the magnetic thermodiffusion especially in the case of the perpendicular aligned magnetic field.

ACKNOWLEDGMENTS

The authors especially thank Dr. Morozov, Professor Blums, and Dr. Mezulis for very helpful discussions in the theoretical as well as in the experimental part of this work. The financial support by the Deutsche Forschungsgemeinschaft in project LA 1182/3 is gratefully acknowledged.

- ¹ A. Mezulis, E. Blums, G. Kronkalns, and M. Maiorov, "Measurements of thermodiffusion of nanoparticles in magnetic colloids," *Latv. J. Phys. Tech. Sci.* **5**, 1–13 (1995).
- ² T. Völker, E. Blums, and S. Odenbach, "Thermodiffusion in magnetic fluids," *J. Magn. Magn. Mater.* **252**, 218–220 (2002).
- ³ L. Sprenger, A. Lange, and S. Odenbach, "Thermodiffusion in concentrated ferrofluids - A review and current experimental and numerical results on non-magnetic thermodiffusion," *Phys. Fluids* **25**, 122002 (2013).
- ⁴ T. Voelker and S. Odenbach, "Thermodiffusion in ferrofluids in the presence of a magnetic field," *Phys. Fluids* **17**, 037104 (2005).
- ⁵ W. Köhler and B. Müller, "Soret and mass diffusion coefficients of toluene/n-hexane mixtures," *J. Chem. Phys.* **103**, 4367–4370 (1995).
- ⁶ J. K. Platten, M. M. Bou-Ali, P. Costesèque, J. F. Dutrieux, W. Köhler, C. Leppla, S. Wiegand, and G. Wittko, "Benchmark values for the Soret, thermal diffusion and diffusion coefficient of three binary organic liquid mixtures," *Philos. Mag.* **83**, 1965–1971 (2003).
- ⁷ T. Völker, E. Blums, and S. Odenbach, "Determination of the Soret coefficient of magnetic particles in a ferrofluid from the steady and unsteady part of the separation curve," *Int. J. Heat Mass Transfer* **47**, 4315–4325 (2004).
- ⁸ J.-C. Bacri, A. Cebers, A. Bourdon, G. Demouchy, B. M. Heegaard, B. Kashevsky, and R. Perzynski, "Transient grating in a ferrofluid under magnetic field: Effect of magnetic interactions on the diffusion coefficient of translation," *Phys. Rev. E* **52**, 3936–3942 (1995).
- ⁹ J.-C. Bacri, A. Cebers, A. Bourdon, G. Demouchy, B. M. Heegaard, and R. Perzynski, "Forced Rayleigh experiment in a magnetic fluid," *Phys. Rev. Lett.* **74**, 5032–5036 (1995).
- ¹⁰ J. Lenglet, A. Bourdon, J.-C. Bacri, and G. Demouchy, "Thermodiffusion in magnetic colloids evidenced and studied by forced Rayleigh scattering experiments," *Phys. Rev. E* **65**, 031408 (2002).
- ¹¹ L. Sprenger, A. Lange, and S. Odenbach, "Thermodiffusion in ferrofluids regarding thermomagnetic convection," *C. R. Mec.* **341**, 429–437 (2013).
- ¹² B. A. Finlayson, "Convective instability of ferromagnetic fluids," *J. Fluid Mech.* **40**, 753–767 (1970).
- ¹³ H. W. Müller and M. Liu, "Structure of ferrofluid dynamics," *Phys. Rev. E* **64**, 061405 (2001).
- ¹⁴ M. Liu, "Hydrodynamic theory of electromagnetic fields in continuous media," *Phys. Rev. Lett.* **70**, 3580–3583 (1993).
- ¹⁵ M. Liu, "Fluid dynamics of colloidal magnetic and electric liquid," *Phys. Rev. Lett.* **74**, 4535–4538 (1995).
- ¹⁶ A. Lange, "Magnetic Soret effect: Application of the ferrofluid dynamics theory," *Phys. Rev. E* **70**, 046308 (2004).
- ¹⁷ A. Lange, personal communication (2010).
- ¹⁸ A. Cebers, "Thermodynamic stability of magnetofluids," *Magneto hydrodynamics* **18**, 137–142 (1982).
- ¹⁹ E. Blums, A. Ceber, and M. Maiorov, *Magnetic Fluids* (Walter de Gruyter & Co., Berlin, 1996).
- ²⁰ R. E. Rosensweig, *Ferrohydrodynamics* (Dover Publications, Mineola, NY, 1997).
- ²¹ S. de Groot and P. Mazur, *Non-Equilibrium Thermodynamics* (North-Holland Publishing Company, Amsterdam, 1962).
- ²² R. W. Chantrell, J. Popplewell, and S. W. Charles, "Measurements of particle size distribution parameters in ferrofluids," *IEEE Trans. Magn.* **14**, 975–977 (1978).
- ²³ K. I. Morozov, "Gradient diffusion in concentrated ferrocolloids under the influence of a magnetic field," *Phys. Rev. E* **53**, 3841–3846 (1996).
- ²⁴ H. Engler, "Parametric modulation of thermomagnetic convection in ferrofluids" (in German), Ph.D. thesis (TU Dresden, 2010).
- ²⁵ E. Blums, S. Odenbach, A. Mezulis, and M. Maiorov, "Soret coefficient of nanoparticles in ferrofluids in the presence of a magnetic field," *Phys. Fluids* **10**, 2155–2163 (1998).
- ²⁶ K. I. Morozov, "The translational and rotational diffusion of colloidal ferroparticles," *J. Magn. Magn. Mater.* **122**, 98–101 (1993).
- ²⁷ L. Sprenger, A. Lange, and S. Odenbach, "Influence of thermodiffusive particle transport on thermomagnetic convection in magnetic fluids," *Magneto hydrodynamics* **49**, 473–478 (2013).
- ²⁸ V. Frishfelds and E. Blums, "Microconvection and mass transfer near bodies in non-uniformly magnetized ferrofluids," *Magneto hydrodynamics* **41**, 361–366 (2005).
- ²⁹ J. D. Anderson, E. Dick, G. Degrez, R. Grundmann, J. Degroote, and J. Vierendeels, *Computational Fluid Dynamics: An Introduction* (Springer-Verlag, Berlin/Heidelberg, 1992).
- ³⁰ M. Schäfer, *Numerics in Mechanical Engineering (in German)* (Springer-Verlag, Berlin/Heidelberg, 1999).
- ³¹ T. Westermann, *Modelling and Simulation (in German)* (Springer-Verlag, Berlin/Heidelberg, 2010).
- ³² T. Völker and S. Odenbach, "The influence of a uniform magnetic field on the Soret coefficient of the magnetic nanoparticles," *Phys. Fluids* **15**, 2198–2207 (2003).
- ³³ A. Zubarev, personal communication (2012).